ARTICLE

Reactive Molecular Dynamics Simulation on Thermal Decomposition of n-Heptane

Juan-qin Li[a*], Fan Wang[b], Xue-ming Cheng[a], Xiang-yuan Li[a]

a. College of Chemical Engineering, Sichuan University, Chengdu 610065, China
b. College of Chemistry, Sichuan University, Chengdu 610065, China

(Dated: Received on December 13, 2012; Accepted on March 25, 2013)

The thermal decomposition of n-heptane is an important process in petroleum industry. The theoretical investigations show that the main products are C_2H_4, H_2, CH_4, and C_3H_6, which agree well with the experimental results. The products populations depend strongly on the temperature. The quantity of ethylene increases quickly as the temperature goes up. The conversion of n-heptane and the mole fraction of primary products from reactive molecular dynamic and chemical kinetic modeling are compared with each other. We also investigated the pre-exponential factor and activation energy for thermal decomposition of n-heptane by kinetic analysis from the reactive force field simulations, which were extracted to be 1.78×10^{14} s^{-1} and 47.32 kcal/mol respectively.

Key words: Chemical kinetic modeling, ReaxFF, n-Heptane, Thermal decomposition

I. INTRODUCTION

During the past decades a large number of works which deal with the thermal decomposition of paraffin hydrocarbons appeared in the literatures [1−4]. The decomposition of hydrocarbons to ethylene, propylene, and 1,3-butadiene is an important process in petroleum industry. n-heptane is an important ingredient in many fuels and produces a large amount of heat when being burned. It has been estimated that among the alkanes from C_5H_{12} to $C_{12}H_{26}$, heptane has the highest conversion ratio and the highest yield of ethylene at about 780 °C [5]. For this reason, n-heptane attracts a lot of attention because of its unique characteristics. An important challenge in developing Scramjet (supersonic combustion ramjet) engine is related to the cooling of the walls of the engine. Especially, as the aircraft flight speed increases to supersonic and hypersonic regimes, the pyrolysis of hydrocarbons existing in Scramjet engine emerging for hypersonic flight is very complicated. Researches focus on the possibility to use the thermal decomposition of a fuel circulating on the metallic material walls of the Scramjet in order to quantify the heat transfer in the cooled structures and the composition of the mixture entering the combustor [6]. Thus, the most desired product of thermal decomposition of fuels is ethylene.

Experimental studies as well as theoretical simulations on the thermal decomposition and catalytic pyrolysis of n-heptane have been carried out extensively in the past years [7−11]. A semi-detailed kinetic scheme for n-heptane oxidation has been developed by Ranzi *et al.* and Curran *et al.* [12, 13]. Come *et al.* have used a computer package to automatically generate the chemical kinetic mechanisms for n-heptane and iso-octane [14]. These researches provided a lot of useful information on the mechanism of decomposition reactions.

Recently, reactive force field (ReaxFF) developed by Duin and co-workers has been used for combustion and decomposition of hydrocarbons [15]. It has been designed to describe the structures and reactions involving non-conjugated, conjugated, and radical containing compounds and, additionally, to describe the dissociation and formation of chemical bonds in relatively large hydrocarbon systems (C_{100+}) [16−19]. Whereas traditional force faults are unable to model chemical reactions because of the requirement of breaking and forming chemical bonds. ReaxFF eschews explicit bonds in favor of bond orders, which allows for continuous bond formation/breaking, and it succeeds in predicting the dynamical and reactive processes in combustion and decomposition of hydrocarbons [15], silicon/silicon oxides [19], and nitramines [20]. These simulations provide valuable insight into the chemical reaction under extreme conditions which is almost impossible in practice.

In order to gain insight into the thermal decomposition of hydrocarbons, we propose here a novel approach to study the thermal decomposition of n-heptane by comparing reactive force field molecular simulation with the chemical kinetic modeling. We have developed a reaction mechanism generator based on reaction class

*Author to whom correspondence should be addressed. E-mail: lijuanqin@scu.edu.cn, Tel.: +86-28-85403537, FAX: +86-28-85407797.

rules to generate reaction mechanism used for chemical kinetic modeling. The code is based on canonical treelike description for molecules and radicals. The mechanism generator can be used directly as an input file to run simulations based on the Chemkin II program [21]. The macroscopic chemical kinetic modeling is able to provide detailed information on conversion rate, product distribution. With the mechanism generator, we obtained a good agreement between the simulated and experimental data. ReaxFF is used to investigate the initial mechanisms of thermal decompositions of *n*-heptane. The results from the two different methods correlate rather well.

II. COMPUTATIONAL DETAILS

A. Reaction mechanism

The kinetic modeling of the hydrocarbon decomposition requires considering thousands of elementary reactions and species. Actually, if the reaction classes are comprehensive and each new species is submitted to the application of all reaction rules, the generic mechanisms are comprehensive. There are several available programs for automatic generation of kinetic mechanisms for the decomposition and oxidation of large hydrocarbons. Pierucci *et al.* give a good summary of the generation codes and conclude that a generation program should have these features in common, one is the existing database storing, for example, the schemes C_0-C_2, the other is the representation of the species [22]. Generating reaction models by computer relies critically on representing chemical species by a notation that gives a complete and unique representation of the arrangement of the atoms and their connectivity (by bonding) to other atoms. Some popular notations and techniques, such as treelike representation, matrix representation, SMILES (simplified molecular input line system) notation have been reported [23−25].

The reaction mechanism generator was developed in our group for automated generation of thermal decomposition reaction mechanisms of large hydrocarbon molecules. In this work, SMILES notation is employed to obtain the unique SMILES notation for one specified species, an algorithm similar to UNIQUE SMILES is adopted. In short, each chemical species is treated as a graph with nodes (atoms) and edges (bonds). All atoms are canonically ranked on the basis of a suitable set of invariant node properties and are labeled numerically. Starting from the lowest ranked atom, a tree (molecular graph) that represents the molecule uniquely can be constructed. The main algorithm of our work is based on the chemical graph theory [26, 27], and the most important section is the reaction rules. The reaction types of large hydrocarbons are limited but should be updated when new species or reactions arise.

In this investigation the reaction mechanism generator will produce two necessary files for chemical kinetic modeling. One is the kinetic data and the other is the thermodynamics data. The former shows the kinetic mechanisms including detailed reactions and its corresponding kinetic parameters, and the latter includes the thermal chemistry parameters of the species involved in these reactions. The associated thermo-chemical data are calculated based on group-additivity method, which has proven to be a reliable approach to estimate thermodynamic properties for stable molecules and radicals [28, 29].

B. Molecular dynamic simulation-reactive force field

ReaxFF was developed to reproduce quantum mechanics (QM) energies for a large variety of reaction pathways involving reaction intermediates and transition statesman [20, 30, 31]. The parameters in ReaxFF are adjusted to reproduce the energetic and reactive surfaces found with QM for a number of prototypical systems and then used for system with sizes far beyond capabilities of present QM calculations [15]. The ReaxFF is based on quantum mechanical computations and uses a general relationship between bond distance and bond energy on one hand and a second relationship between bond order and bond energy on the other hand. The total energy is divided into various partial energy contributions, as demonstrated by Eq.(1) [15].

$$E_{\text{system}} = E_{\text{bond}} + E_{\text{over}} + E_{\text{under}} + E_{\text{val}} + E_{\text{pen}} + E_{\text{tors}} + E_{\text{conj}} + E_{\text{vdWaals}} + E_{\text{Coulomb}} \quad (1)$$

$$E_{\text{bond}} = -D_{\text{e}}\text{BO}_{ij} \exp\left[p_{\text{be},1}(1 - \text{BO}_{ij}^{p_{\text{be},1}})\right] \quad (2)$$

here E_{bond} denotes the bond energy, which is a function of bond order (BO_{ij}). E_{over} and E_{under} denote the over- and under-coordinated atom in the energy contribution, respectively. E_{val}, E_{pen}, E_{tors}, E_{conj}, E_{vdWaals}, and E_{Coulomb} denote the valence angle term, penalty energy, torsion energy, conjugation effects to molecular energy, non-bonded van der Waals interaction, and coulomb interaction, respectively.

A number of force fields for hydrocarbons, such as MM3 [32−35], DREIDING [36], and UFF [37], can provide accurate predictions of geometries, conformational energy differences, heats of formation, and charge equilibrations. However, these force fields do not describe the chemical reactivity. ReaxFF, on the other hand, can be applied to the study of the high-temperature dynamics of chemically reactive systems, providing an atomistic-scale description on the decomposition of high-energy materials [20, 38−41]. ReaxFF method has been successfully employed to investigate the explosion of nitromethane [42, 43], thermal decomposition of cyclic-$[CH_2N(NO_2)]_3$ [30], poly(dimethylsiloxane) and JP-10 fuel [44]. The ReaxFF proposed a transferable force field that can describe the energy surfaces and condition changes associated with reactions while simultaneously describing ground state structures correctly.

DOI:10.1063/1674-0068/26/02/211-219

Based on the ReaxFF, we investigated the thermal decomposition of n-heptane with reactive molecular dynamics (MD). All of the MD simulations were performed with a constant number of atoms (N) in a constant volume (V) with control of the temperature (T) using a thermostat and this condition is designated as NVT. In order to investigate the decomposition of n-heptane, we placed 20 n-heptane molecules in a unit cell measuring 26 Å×26 Å×14 Å. The energy of the system was minimized using low temperature (5 K) MD and then equilibrated with NVT-MD for 10 ps at 1500 K using a time step of 0.1 fs. The temperature was controlled with Berendsen thermostat using a 0.2 ps damping constant. The equilibrated system had a density of 0.35 g/cm^3, and a pressure of approximately 6 MPa, which can easily occur in many reactive processes, including rocket engines and shock-induced reactions.

After equilibration, 10 unique starting configurations were collected. The results from these 10 simulations were averaged to study the kinetics of decomposition. The MD simulations are performed at temperatures of 2000, 2100, 2200, 2300, 2400, and 2500 K for a total simulation time of 500 ps with a step length of 0.1 fs. The overall product distributions varing as a function of the temperature are studied. We analyzed the intermediates and products formed during the MD simulation using a 0.3 bond-order cutoff for molecular recognition. The choice of bond-order cutoff does not affect the simulation itself but only affects its interpretation in terms of chemical components. To reduce the total simulation time, the MD simulations are performed at high temperatures, although the real reactions carried out at much lower temperatures around 900 K.

III. RESULTS AND DISCUSSION

A. The product distribution of n-heptane from chemical kinetic and reactive MD simulations

Experiments on the thermal decomposition of n-heptane have been carried out at about 1000 K, and it has been reported that at a given conversion ratio the yield of the products is constant, and will be less affected by temperature [45]. In rocket engines, high temperature and pressure are highly desirable for good performance as this permitting a long nozzle to be fitted to the engine, which gives higher exhaust speeds and better thermodynamic efficiency as well. We performed both the reactive molecular dynamics simulation with ReaxFF and the kinetics simulation with Chemkin II at high temperatures and investigated the thermal decomposition of n-heptane from 2000 K to 2500 K at an interval of 100 K within 500 ps.

We investigated the product distribution of n-heptane thermal decomposition by the newly developed mechanism. The mechanism is made up of 557 elementary reactions and 140 species. The chemical kinetic

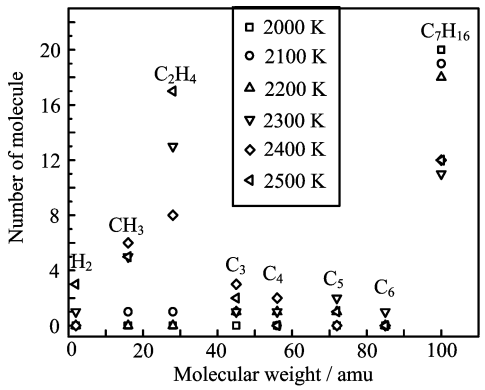

FIG. 1 Superposition of final product distribution at t=500 ps at various temperatures using ReaxFF simulations.

modeling is carried out in a closed, homogeneous reactor under 6.0 MPa with Chemkin II package. The yields of C_2H_4, CH_4, C_3H_6, and H_2 are obtained at the different temperatures. The results shown in Fig.1 indicate that the product yields increase with temperature. Chemkin simulation results also demonstrate that the amount of alkenes is much more than that of alkanes, which agrees well with the experiment [10]. The simulation also shows that the C_2H_4 is the main decomposition product, whose yield is much higher than other products. Besides C_2H_4, a significant amount of C_3H_6, CH_4 and H_2 are also produced.

To gain insight into the relationship between temperature and product distribution, we investigated the product distributions in the temperature range of 2000−2500 K. When the temperature increases from 2000 K to 2500 K, the amount of unreacted n-heptane decreases, accompanied by an increase of the quantities of C_2, C_3, C_4, C_5 and C_6 hydrocarbons (see Fig.1). It shows that the equilibrium population of C_2H_4 and H_2 depends strongly on temperature. It is interesting to note that the quantities of CH_3, C_3 and C_4 species, and the C_5 and C_6 species reach the maximum at 2400 or 2300 K, respectively. This indicates that these species are unstable at high temperatures. More detailed investigation by Chemkin II reveals that the increase of the temperature will accelerate the forward reaction rate of the reversible reaction $C_2H_4+CH_3\cdot \rightleftharpoons CH_4+C_2H_3\cdot$, leading to the increasing consumption of ethylene.

From Fig.1, we can see that high temperature will speed up the decomposition process. Pant and coworkers found that when the conversion ratio was given the temperatures would less affect the product yields [45]. The effect of temperature on the product yields versus the conversion ratio was investigated. Figure 2 shows the yield of the major products (*e.g.* ethylene and hydrogen) as functions of the conversion ratio. We find that when the conversion ratio increases, the product yields increase. Our computational results show that, in the temperature range, at the given conversion ratio,

DOI:10.1063/1674-0068/26/02/211-219

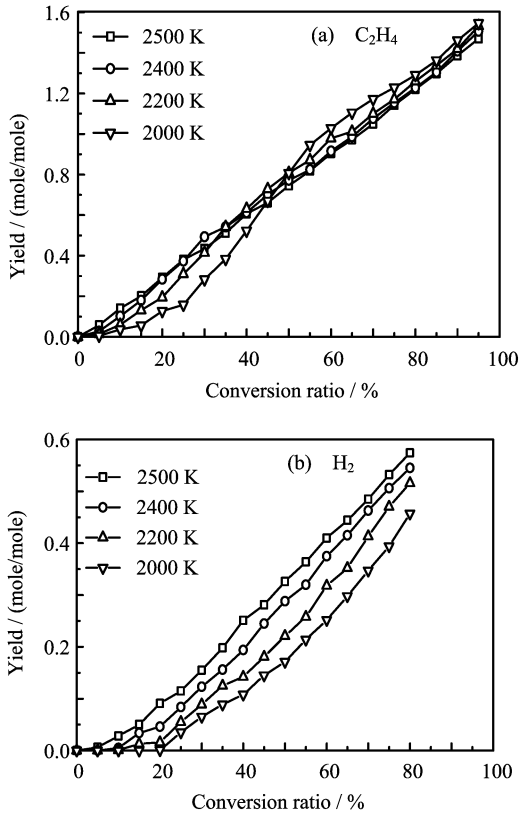

FIG. 2 Plots of product yield against conversion ratio at various temperatures.

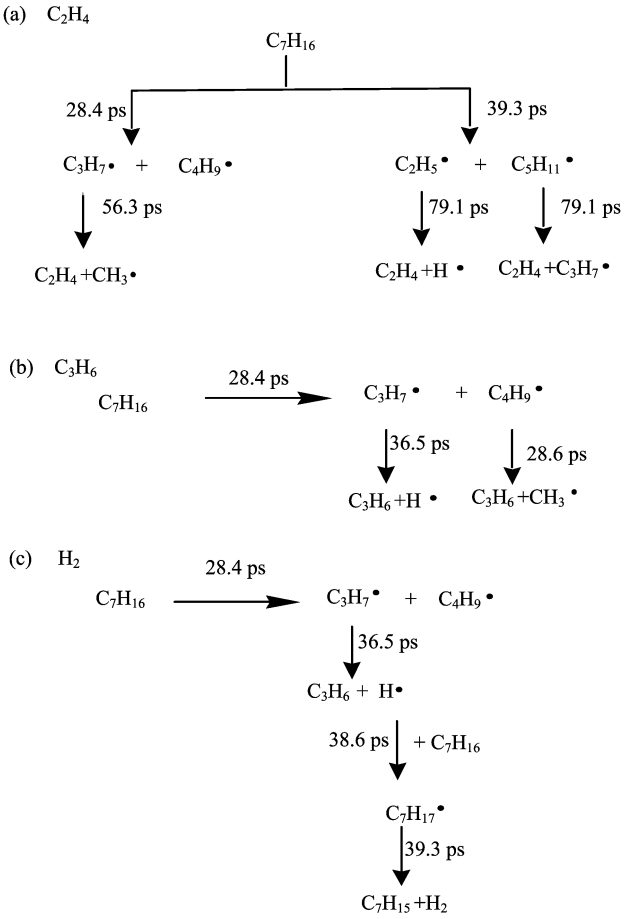

FIG. 3 Initiation reaction mechanism of the decomposition of *n*-heptane revealed by NVT-MD at 2200 K.

the yield of the product has little change. This agrees well with the experimental results [45]. The yield of hydrogen is significantly lower than that of ethylene, so the result from Fig.2(b) is not as good as that from Fig.2(a).

The reaction mechanisms of decomposition processes of the *n*-heptane molecules at 2200 K based on reactive MD simulation are explicitly shown in Fig.3, through which we can obtain the framework of the main product channels.

The major product ethylene emerges through two ways, one is the *n*-heptane cleavage to butyl and propyl radicals, which decomposes to give C_2H_4 and CH_3 radicals, the other way is that the *n*-heptane cracks to ethyl and pentyl radicals at first, then the pentyl radical decomposes to bring forth ethylene and propyl radicals, and ultimately, the propyl radicals cleavage to allyl radical and hydrogen follows through dehydrogenation. It is well known that *n*-butyl radical will decompose to produce C_2H_4 and C_2H_5 radical through β-scission, but in this simulation C_2H_4 is not produced from this way. It should be noted that *sec*-butyl radical, on the other hand, is prone to generate C_3H_6 and CH_3 radical. The *sec*-butyl radical is more stable than the *n*-butyl radical, and the isomerism could take place between them. This means the C_4H_9 radical in Fig.3 (a) and (b) is actually *sec*-butyl radical. Through ReaxFF simulation we can also explain why the ethylene appears earlier than hydrogen. The other pathway of the main product as propylene and hydrogen are also given in Fig.3. We can find out that formation of H radical from C_3H_7 radical. When the temperature is not very high, the reaction rate of the β-scission is larger than the H abstraction from alkyl radicals. However, the situation could be different at the high temperature. From kinetic parameters in the following [46, 47]:

$$\mathrm{C_3H_7} \rightarrow \mathrm{CH_3}+\mathrm{C_2H_4}$$
$$k_1 = 8.0 \times 10^{12} \exp\left(\frac{-16622}{T}\right)$$
$$\mathrm{C_3H_7} \rightarrow \mathrm{H} + \mathrm{C_3H_6}$$
$$k_2 = 1.41 \times 10^{-3} T^{4.20} \exp\left(\frac{-4378}{T}\right)$$

one can readily obtain rate constant for these two reactions at the temperate of 2200 K, k_1=4.18×10^9 s^{-1} and k_2=2.10×10^{10} s^{-1} . This means it is prone to generate C_3H_6 and CH_3 radical as listed in Fig.3(b)).

At 2200 K simulation, C_2H_4 arises at 56.3 ps, and C_4H_8 and C_2H_6 are the main products within the

DOI:10.1063/1674-0068/26/02/211-219

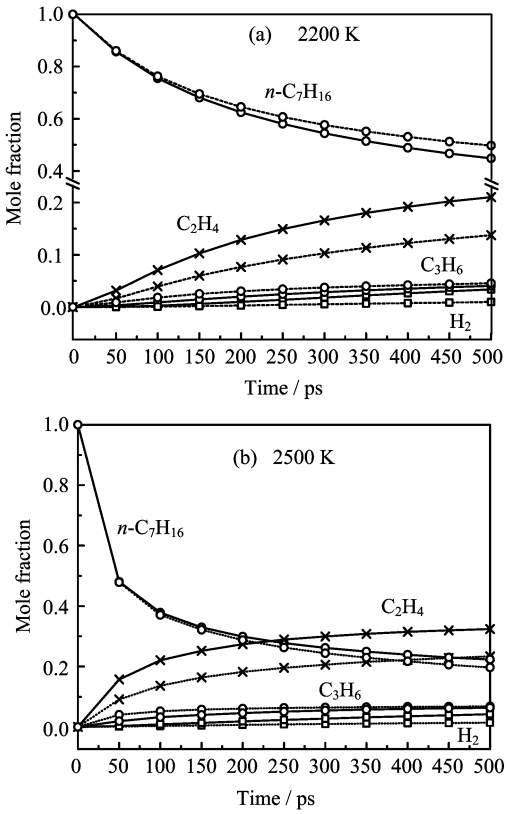

FIG. 4 Decomposition product distributions from ReaxFF MD (dotted lines) and Chemkin II (solid lines) as a function of simulation time at 2200 and 2500 K. Only major products are shown explicitly.

simulation time. The thermal decomposition of n-heptane proceeds according to the following steps: $C_7H_{16} \rightarrow C_4H_9\cdot + C_3H_7\cdot$, and then $C_4H_9\cdot \rightarrow C_4H_8 + H\cdot$, and $C_7H_{16} + H\cdot \rightarrow C_7H_{17}\cdot$, $C_7H_{17}\cdot \rightarrow C_5H_{11}\cdot + C_2H_6$. In Fig.4(a), the ReaxFF results are compared with those from Chemkin II method. The yields of ethane and butylenes are in reasonable agreement.

In ReaxFF simulation, C_2H_4 and H_2 appear at 9.6 and 16.4 ps at 2500 K, respectively. The unimolecular decomposition of the n-heptane undergoes a stepwise mechanism. At first, the cleavage occurs between the C−C bonds, producing the given alkyl radical, and then further cleavage happens in the alkyl radicals, followed by production of ethylene, methyl radical, n-propyl radical and hydrogen molecule. When n-heptane decomposes, new fragments are formed. The decomposition is faster when the temperature increases. It is obvious that the higher temperature is favor for the decomposition reaction, and can shorten the time at which n-heptane begins to decompose.

The mole fraction as a function of simulation time at 2200 and 2500 K are shown in Fig.4 both from ReaxFF and Chemkin II. Although ReaxFF is the microscopic molecular dynamics simulation method while Chemkin II performs a macroscopic kinetics simulation, we can find the consistent trends on the product distributions. The two methods give the similar results about the product distribution. Comparing Fig.4 (a) and (b), we can see that the microscopic molecular dynamics simulation and the macroscopic kinetics simulation match very well. Compared with the result at 2200 K, the n-heptane decomposes more quickly at 2500 K, leading to final products C_2H_4, CH_3 radical, and H_2 along with other intermediates. This suggests that the higher temperature favors the formation of the desired product C_2H_4. Within the simulation time, the product distributions are deeply affected by temperature, and there is no ethylene, methyl radical and hydrogen at 2200 K within the simulation time. Obviously, the conversion of n-heptane at 2500 K is much larger than that of 2200 K.

B. Comparisons between chemical kinetic modeling and reactive MD simulations

A comparative study of main product distribution from chemical kinetic modeling and ReaxFF simulation is of particular interest for two reasons. Firstly, chemical kinetic modeling of thermal decomposition of n-heptane is performed by using the Chemkin II package, which is based on the reaction mechanism generated by the newly developed mechanism generator. The results from Chemkin can be verified by that of the ReaxFF methods at high temperature. Secondly, the consistent prediction for n-heptane decomposition by both reactive molecular dynamic simulation and chemical kinetic modeling provides a validation between the micro- and macro-simulations.

The mole fraction of individual species as a function of simulation time is shown in Fig.5. Through the two kinds of simulation we find that the n-heptane decomposed relatively fast at the beginning. It can be seen from this figure that results on the trend of the main product distributions of these two simulations agree reasonably well with each other. We assume that if more n-heptane molecules can be used in the ReaxFF simulation, better agreement will be achieved. A noticeable difference between results of the two simulations appears at the initial time and this difference decreases at later simulation times. Difference in the initial time may be related to the fact that reactions are not yet stable at the beginning and the limited n-heptane molecules selected in the ReaxFF simulation. Simulation results on production yields of ethylene, methyl radical and hydrogen indicate that the reaction mechanism generated by our work is able to provide reasonable results.

C. The reaction mechanism of thermal decomposition of n-heptane

We analyzed the chemical reaction mechanism of the thermal decomposition of n-heptane at the studied con-

DOI:10.1063/1674-0068/26/02/211-219

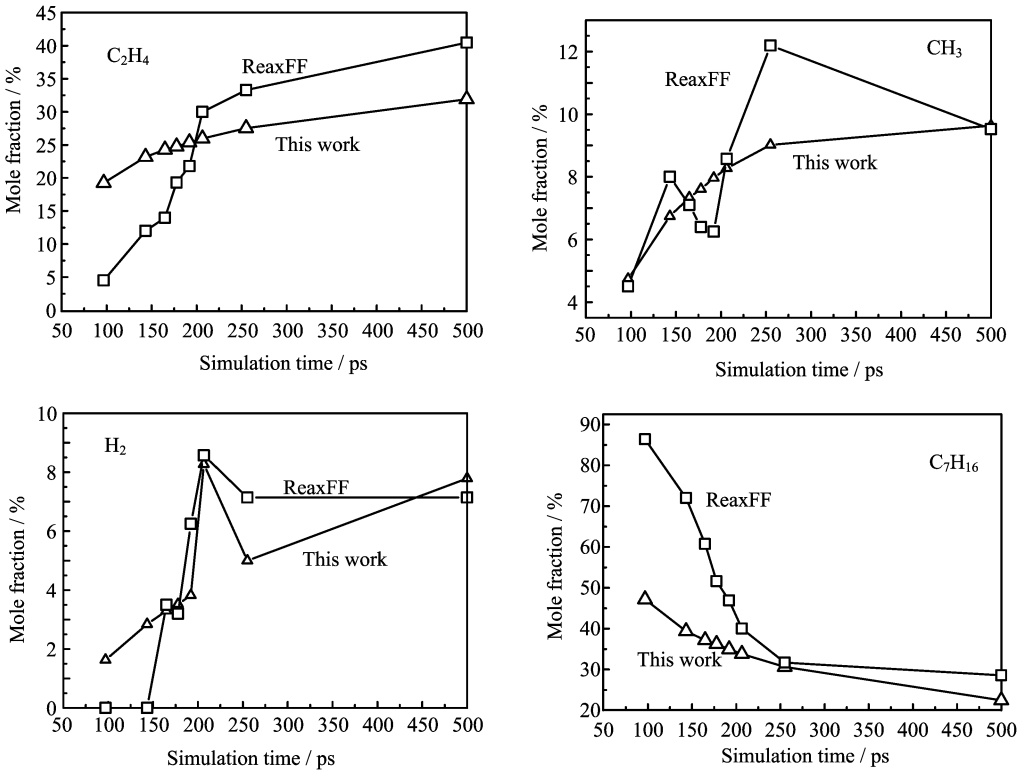

FIG. 5 Mole fraction of the dominant products at various simulation time by ReaxFF and this work.

ditions and found that C_2H_4 is the dominant product. The results from ReaxFF simulation are shown in Fig.5. The main intermediates obtained during the decomposition include C_2H_5, C_3H_7, C_4H_9, and C_5H_{11} radicals. The decomposition mechanism is investigated by tracking the trajectories of species in the decomposition. We analyzed the reaction mechanism for the decomposition of *n*-heptane at 2500 K and found that the C_3H_7 radical is mainly formed via C−C bond rupture during the early stage, and the small alkene molecules occur subsequently. The major route for the formation of ethylene is $C_7H_{16}\rightarrow C_3H_7\cdot + C_4H_9\cdot$, and then $C_4H_9\cdot\rightarrow C_2H_5\cdot + C_2H_4$, $C_3H_7\cdot\rightarrow CH_3\cdot + C_2H_4$. This result is consistent with that from the literature [12]. The *n*-heptane cracks to ethyl and pentyl radicals firstly, and then the pentyl radical cracks again to form ethylene, which is shown as process II in Fig.6. Another way of *n*-heptane decomposition is to generate methyl radical and hexyl radical, and the hexyl radical cleaves to ethylene and the corresponding radicals. Through the investigation of the ReaxFF simulation we find that the hydrogen abstraction reaction can also occur during the *n*-heptane decomposition. These validations provide support for the reaction mechanism described in this work.

From the ReaxFF simulation, we can obtain the simple and clear logical framework of the *n*-heptane thermal decomposition. The *n*-heptane decomposition was further analyzed by Chemkin II in order to determine the principle paths through our new mechanism. The primary paths of *n*-heptane decomposition from Chemkin II are shown in Fig.7. The values on the arrow indicate the percentage of the reaction. A comparison with Fig.6 shows that the two different simulation methods are fully consistent. On one hand, the results demonstrate that the macro- and micro-simulation modeling can be consistent, on the other hand, ReaxFF can provide a way for the validation of complex kinetics mechanism for decomposition of hydrocarbons. Through the two different simulations, a reasonable and clear pathway of the *n*-heptane thermal decomposition is possible. The primary paths of the decomposition of *n*-heptane are via C−C bond rupture. The results can also be used to assist the construction of reduced reaction mechanism for hydrocarbon pyrolysis, which could be useful in engineering application and the computational fluid dynamics.

D. Kinetic analysis

Aside from validating the reaction path of *n*-heptane, it is also of interest to assess the reliability of the decomposition mechanism generated by our work in low temperature environments. In order to validate the new mechanism, it is necessary to carry out comparisons of others mechanisms and the experimental results in the literatures. In the present study the mechanism is vali-

DOI:10.1063/1674-0068/26/02/211-219

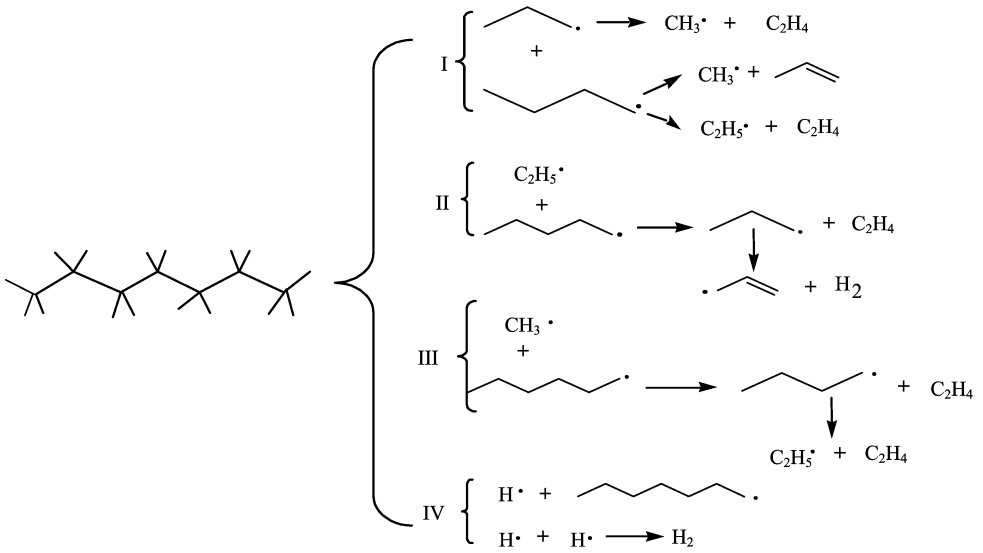

FIG. 6 The main initial mechanism of n-heptane decomposition by ReaxFF.

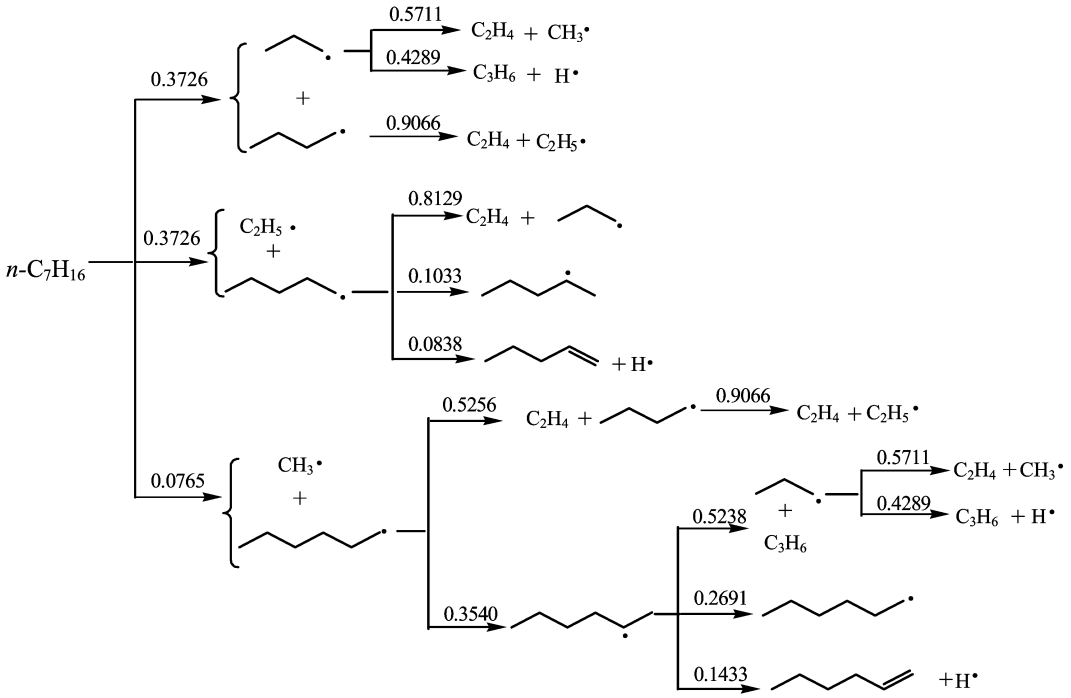

FIG. 7 The main pathways of n-heptane decomposition by Chemkin II simulation. The values on the arrow indicate the percentage of the reaction.

dated by two ways. (i) The experimental decomposition are always carried out at relatively low temperature, the simulation results will be validated by experimental data obtained in stirred reactors and theoretical simulation by Curran, Ranzi, and Muller. The experiment is carried out from 1120 K to 1370 K with a step of 25 K. Details of the experimental apparatus are provided by Levuch *et al.* [48]. (ii) Due to the lack of direct experimental information at high temperature, the calculated results from our work will be compared with other theoretical simulations.

In this work the decomposition of n-heptane is in a jet-stirred reactor within a temperature range of 1120−1370 K. The simulation results among this temperature region are shown in Fig.8. We can see that the results from our work are also consistent with those of other simulation and the rate constant increases with increasing temperature. The theoretical simulation agrees well with experimental data. However, there are differences between the different mechanisms, and the devia-

DOI:10.1063/1674-0068/26/02/211-219

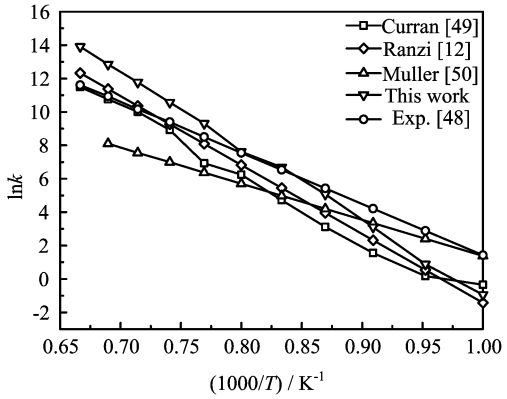

FIG. 8 Kinetics analysis of n-heptane from the different mechanisms in the temperature region of 1000−1500 K.

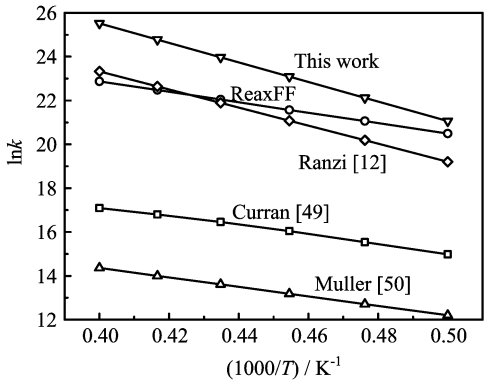

FIG. 9 Kinetic analysis of n-heptane from the different mechanisms in the temperature region of 2000−2500 K.

tion from theoretical calculation and experimental data are relatively large. The investigation results indicate that the new mechanism is relatively reasonable.

Since the kinetic data of the high temperature are not available from the experiment, the decomposition reaction rates are contrasted with the results from ReaxFF simulations. The overall kinetics of thermal decomposition of n-heptane by ReaxFF simulation was determined by the non-linear regression analysis. The temperature range of decomposition is from 2000 K to 2500 K in 100 K steps. The simulations were carried out for 100 ps at each temperature with a 0.1 fs step. The first order kinetics fits reasonably well to a single Arrhenius function, allowing us to extract an effective activation energy $E_{\rm a}$ and pre-exponential factor A. Linear fitting results show that the decomposition of n-heptane leads to $E_{\rm a}$ and A are 47.32 kcal/mol and 11.78×10^{13} s^{-1}, respectively.

The results are also mutually compared with that of Curran, Ranzi, and Muller mechanisms [12, 49, 50]. Figure 9 shows that the fitted rate constants at high temperature in this work are slightly larger than the ReaxFF method and the simulation results from Curran and Muller mechanisms have a relatively large deviation from ReaxFF simulation results. This is because of the distinct kinetic parameters from different decomposition mechanisms, where the rate constants of the elementary reactions of the n-heptane decomposition from this work and Refs. [12, 49, 50] are different from each other. A further analysis indicate that A and $E_{\rm a}$ of Muller's simulation are 1.0×10^{10} and 180 kJ/mol, respectively [50]. Therefore, in the ln$k$-T diagrams the corresponding slope is relatively small. So you can see at the low temperature the simulation results matched well with the experimental data. However, at the high temperature the simulation results have a large deviation from the ReaxFF simulation results. For Curran's mechanism, some adjustments have been made to the kinetic parameters; the temperature index was fixed to a large negative value of −17.60, and the activation energy becomes relatively small to be 120.4 kJ/mol [50]. So in the high temperature the corresponding simulation results have a large deviation from the ReaxFF simulation results. Therefore, this data are reasonable in the case of low temperature, and at the high temperature the reaction rate will be underestimated. The rate constants fitted from our work are little higher than that from ReaxFF simulation.

IV. CONCLUSION

A new developed kinetic generator of hydrocarbons decomposition has been described. Based on the kinetic and thermodynamic data, chemical kinetic simulations of the n-heptane decomposition have been carried out, in parallel with Reactive force field MD simulations. The decomposition of n-heptane is discussed in the temperature range of 2000−2500 K, and the detailed analyses are made on the results of 2200 and 2500 K. The simulation results indicate that increasing the temperature will favor the decomposition of n-heptane and improve the yield of ethylene. Through the investigation we found that at a given conversion ratio, the temperature has little effect on the product yield. The mole fractions of the dominant products changing with the simulation time have also been investigated. It can be seen that the ReaxFF and the simulation give very similar results, especially for the stable intermediates. The chemical kinetic modeling and Reactive MD both propose a reasonable reaction pathway for the decomposition of n-heptane. The results from the two methods agree well. The mutual checks support the simulation results of this work to a certain extent.

This work is validated through the experimental and theoretical comparisons. The activation energy and pre-exponential factor were obtained from the ReaxFF study of kinetic analysis. These results should be considered as a contribution to produce the mechanism for thermal decomposition of alkanes. The kinetic analysis shows that both at the low and high temperature the

DOI:10.1063/1674-0068/26/02/211-219

simulation results from this work are reasonable, and the new mechanism is reliable.

V. ACKNOWLEDGMENT

This work was supported by the National Natural Science Foundation of China (No.21103117).

[1] F. Behar, F. Lorant, H. Budzinski, and E. Desavis, Energy Fuels **16**, 831 (2002).
[2] R. A. Wolf, R. J. Trocino, W. R. Rozich, I. C. Sabeta, and R. J. Ordway, J. Org. Chem. **63**, 3814 (1998).
[3] J. Yu and S. Eser, Ind. Eng. Chem. Res. **37**, 4601 (1998).
[4] J. Yu and S. Eser, Ind. Eng. Chem. Res. **36**, 585 (1997).
[5] M. Bajus, V. Vesely, P. A. Leclercq, and J. A. Rijks, Ind. Eng. Chem. Prod. Res. Dev. **18**, 30 (1979).
[6] K. D. Dahm, P. S. Virk, R. Bounaceur, F. Battin-Leclerc, P. M. Marquaire, R. Fournet, E. Daniau, and M. Bouchez, J. Anal. Appl. Pyrolysis **71**, 865 (2004).
[7] B. A. Watson, M. T. Klein, and R. H. Harding, Ind. Eng. Chem. Res. **35**, 1506 (1996).
[8] K. K. Pant and D. Kunzru, Ind. Eng. Chem. Res. **36**, 2059 (1997).
[9] C. S. McEnally, D. M. Ciuparu, and L. D. Pfefferle, Combust. Flame **134**, 339 (2003).
[10] W. G. Appleby, W. H. Avery, and W. K. Meerbott, J. Am. Chem. Soc. **69**, 2279 (1947).
[11] J. X. Ding, L. Zhang, and K. L. Han, Combust. Flame **158**, 2314 (2011).
[12] E. Ranzi, P. Gaffuri, T. Faravelli, and A. Sogaro, Combust. Flame **102**, 179 (1995).
[13] H. J. Curran, P. Gaffuri, W. J. Pitz, and C. K. Westbrook, Combust. Flame **114**, 149 (1998).
[14] G. M. Come, V. Warth, P. A. Glaude, and R. Fournet, *26th Symposium* (*International*) on Combustion. Pittsburgh: the Combustion Institute, 755 (2006).
[15] A. C. T. van Duin, S. Dasgupta, F. Lorant, and W. A. Goddard III, J. Phys. Chem. A **105**, 9396 (2001).
[16] L. Liu, C. Bai, H. Sun, and W. A. Goddard III, J. Phys. Chem. A **115**, 4941 (2011).
[17] L. Zhang, S. V. Zybin, and W. A. Goddard III, J. Phys. Chem. B **113**, 10770 (2009).
[18] K. Chenoweth, A. C. T. van Duin, and W. A. Goddard III, J. Phys. Chem. A **112**, 1040 (2008)
[19] A. C. T. van Duin, A. Strachan, S. Stewman, Q. S. Zhang, X. Xu, and W. A. Goddard III, J. Phys. Chem. A **107**, 3803 (2003).
[20] A. Strachan, A. C. T. van Duin, D. Chakraborty, S. Dasgupta, and W. A. Goddard III, Phys. Rev. Lett. **91**, 098301 (2003).
[21] R. J. Kee, F. M. Rupley, and J. A. Miller, *Sandia National Laboratories Report No. SAND-89-8009B*, Albuquerque, NM: Sandia National Laboratories, (1989).
[22] R. E. Del and L. Pierucci, IEEE Commun. Mag. **40**, 150 (2002).
[23] D. Weininger, J. Chem. Inf. Comput. Sci. **28**, 31 (1988).
[24] D. Weininger, A. Weininger, and J. L. Weininger, J. Chem. Inf. Comput. Sci. **29**, 97 (1989).
[25] D. Weininger, J. Chem. Inf. Comput. Sci. **30**, 237 (1990).
[26] A. T. Balaban, J. Chem. Inf. Comput. Sci. **25**, 334 (1985).
[27] V. Warth, L. F. Battin, R. Fournet, P. A. Glaude, G. M. Come, and G. Scacchi, Comput. Chem. **24**, 541 (2000).
[28] E. R. Ritter and J. W. Bozzelli, Int. J. Chem. Kinet. **23**, 767 (1991).
[29] T. H. Lay, J. W. Bozzelli, and A. M. Dean, J. Phys. Chem. **99**, 14514 (1995).
[30] A. Strachan, E. M. Kober, A. C. T. van Duin, J. Oxgaard, and W. A. Goddard III, J. Chem. Phys. **122**, 054502 (2005).
[31] K. D. Nielson, A. C. T. van Duin, J. Oxgaard, W. Q. Deng, and W. A. Goddard III, J. Phys. Chem. A **109**, 493 (2005).
[32] T. Maxim, A. Saeed, and S. R. Tafipolsky, J. Comput. Chem. **28**, 1169 (2007).
[33] N. L. Allinger, M. Rahman, and J. H. Lii, J. Am. Chem. Soc. **112**, 8293 (1990).
[34] J. H. Lii and N. L. Allinger, J. Comp. Chem. **12**, 186 (1991).
[35] J. H. Lii and N. L. Allinger, J. Comp. Chem. **19**, 1001 (1998).
[36] E. Buncel, A. J. Mckerrow, and P. M. Kazmaier, Mol. Cryst. Liq. Cryst. **211**, 415 (1992).
[37] A. K. Rappe, C. J. Casewit, K. S. Colwell, W. A. Goddard III, and W. M. Skiff, J. Am. Chem. Soc. **114**, 10024 (1992).
[38] I. Rosenblum, J. Adler, and S. Brandon, Int. J. Mod. Phys. C **10**, 189 (1999).
[39] C. Bai, L.Liu, and H. Sun, J. Phys. Chem. C **116**, 7029 (2012).
[40] K. Chenoweth, S. Cheung, A. C. T. van Duin, W. A. Goddard III, and E. M. Kober, J. Am. Chem. Soc. **127**, 7192 (2005).
[41] S. Cheung, W. Q. Deng, A. C. T. van Duin, and W. A. Goddard III, J. Phys. Chem. A **109**, 851 (2005).
[42] N. Rom, S. V. Zybin, A. C. T. van Duin, W. A. Goddard III, Y. Zeiri, G. Katz, and R. Kosloff, J. Phys. Chem. A **115**, 10181 (2011).
[43] S. P. Han, A. C. T. van Duin, W. A. Goddard III, and A. Strachan, J. Phys. Chem. B **115**, 6534 (2011).
[44] K. Chenoweth, A. C. T. van Duin, S. Dasgupta, and W. A. Goddard III, J. Phys. Chem. A **113**, 1740 (2009).
[45] K. K. Pant and D. Kunzru, J. Anal. Appl. Pyrolysis **36**, 103 (1996).
[46] M. Nehse, J. Warnatz, and C. Chevalier, *26th Symposium* (*International*) *on Combustion*. Pittsburgh: The Combustion Institute, 773 (1996).
[47] R. Fournet, F. Battin-Leclerc, P. A. Glaude, B. Judenherg, V. Warth, G. M. Come, G. Scacchi, A. Ristori, G. Pengloan, P. Dagaut, and M. Cathonnet, Int. J. Chem. Kinet. **33**, 574 (2001).
[48] S. S. Levuch, A. Z. Savchenkov, S. S. Abadzhev, and V. U. Shevchuk, http://kinetics.nist.gov/kinetics/Detail?id=1970LEV/SAV656:3
[49] U. C. Muller and N. Peters, *24th Symposium (International) on Combustion*, The Combustión Institute, 24, 777 (1992).
[50] H. J. Curran, P. Gaffuri, W. J. Pitz, and C. K. Westbrook, Combust. Flame **129**, 253 (2002).

DOI:10.1063/1674-0068/26/02/211-219